Egyptian Journal of Medical Research

Print ISSN: 2682-4396 / Online ISSN: 2682-440X

The Role of Advanced New MRI Parameters in Cardiomyopathies

Wesam Emam Aly El- Mozy[a], Ahmed Hesham Said[b], Esraa Abd El- Latief Shabaan Abd El-Latief[c] , Naglaa Ezzat Abd El- Mageed[b]

[a] Radiodiagnosis, Cairo University, Egypt

[b] Radiodiagnosis, Beni-Suef University, Egypt

[c] M.B.B.Ch., Diploma degree, Beni-Suef University, Egypt

Article Info

Corresponding Author:

Esraa Abd El- Latief Shabaan

esraa.elamairy@gmail.com

Keywords

Cardiac magnetic resonance imaging

Cardiomyopathies

T1 mapping

Strain analysis

Feature tracking CMR

Late gadolinium enhancement,

HCM

Ischemic cardiomyopathy

Non-ischemic cardiomyopathy

ARVC

Padua criteria

Abstract

Background: Cardiac magnetic resonance imaging (CMR) has made major inroads in the new millennium in diagnosing and assessing the prognosis for patients with cardiomyopathies. **Aim:** The study aimed to demonstrate MRI characteristics of different types of cardiomyopathies by using MRI parameters of myocardial tissue characterization (T1 mapping & ECV) and strain analysis. **Methods:** This was a retrospective study conducted on a total of 130 cases with free distribution from men, women and children at Aswan Heart Center from January 2021 to January 2023. Echocardiography confirmed the diagnosis of cardiomyopathy in one hundred of them. We grouped them as 30 patients in the DCM group, 27 patients in the ICM group, 31 patients in the HCM group, and 12 patients from other types (RCM, ARVD, and LVNC). The other thirty people represented controls (A part from health volunteer program at Aswan Heart Center). Results: Statistically significant T1 mapping values at basal inferior, basal inferolateral and mid inferoseptal segments in the ICM group and basal inferior

segments in the DCM group. Statistically significant global Circumferential, Radial and Longitudinal strain analysis in the ICM, DCM and Others groups, and only global longitudinal strain analysis in the HCM group.

1. Introduction:

For more than 30 years, the term "cardiomyopathies" has been used to describe disorders of the heart with particular morphological and physiological characteristics. The purpose of this statement is to update the classification system for cardiomyopathies to ensure its continued utility in everyday clinical practice.

Cardiovascular magnetic resonance imaging (CMR, also known as cardiac MRI), is a medical imaging technology capable of non-invasive assessment of the function and structure of the cardiovascular system **(1).**

Conventional MRI sequences are adapted for cardiac imaging by using ECG gating and high temporal resolution protocols **(1).**

Cardiac MRI approaches are mostly based on fast gradient-echo pulse sequences, which achieve synthetic "cine" representations of an average cardiac cycle using retrospective electrocardiogram (ECG) gating concepts. On the other hand, cardiac function and flow represent dynamic processes that are affected by a variety of physiologic influences such as respiration, blood pressure, heart rate, exercise, or medication **(2)**.

These limitations may now be overcome by recent advances in real-time MRI that allow for direct monitoring of cardiovascular functions without ECG synchronization and during free breathing. The method proposed here relies on nonlinear inversion (NLINV) reconstructions of gradient-echo MRI datasets and provides a series of high-quality images, i.e., MRI movies, with individual imaging times as short as 20 minutes **(3).**

CMR with native T1 mapping offers a unique noninvasive way to quantify myocardial diffused fibrosis and measure extracellular volume (ECV).

The study aimed to demonstrate the MRI characteristics of different types of cardiomyopathies by using MRI parameters for myocardial tissue characterization (T1 mapping & ECV) and strain analysis.

2. Patients and Methods:

This was a retrospective study conducted on a 130 cases with free distribution from Egyptian men, women and children (60 male, 52 female and 18 child) from different age groups and cities of Egypt at Aswan Heart Center- in Upper Egypt between January 2021 and January 2023. All their data was collected from their files on Paxera Ultima workspace:

name, age, date of birth, address, phone number and identity number. MRI examination, scanned intravenous contrast consent, radiology nursing assessment and order entry form, previous medical history, labs, Echo examination, other diagnostic examinations, and any special medical recommendations were obtained.

Echocardiography confirmed the diagnosis of cardiomyopathy in one hundred of them and the radiologists were aware about that at time of MRI examination.

We grouped them as 30 patients in the DCM group, 27 patients in the ICM group, 31 patients in the HCM group, and 12 patients from other types (RCM, ARVD, and LVNC) in the other group. The other thirty people represented controls (A part from health volunteers program at Aswan Heart Center).

Inclusion criteria: Patients had cardiomyopathy diagnosed by echocardiography and radiologists were aware about that at time of MRI examination.

Exclusion criteria: For both cases and controls: Clinical morbidity precluding induction of anesthesia throughout an examination in uncooperative individuals who require sedation; those who had contrast material contraindications and pregnant females; those who have absolute contraindications to MRI, such as a cardiac pacemaker, intraocular metallic foreign body, claustrophobia, etc.

Methods:

Upon the Ethical Committee, the faculty of Medicine Beni- Suef University's approval no. **FMBSUREC/06122020/Abd El-Latief** was granted.

Magnetic Resonance Images:

Using a phased-array cardiac coil, MRI scans were taken on a 1.5 T Siemens Aera from Germany and a 1.5 T Philips Achieve from the United Kingdom.

Using Philips Achieve workstations from the United Kingdom for Tissue mapping and function data.

Using Segment CMR medviso AB Griffelvagen, Lund, Sweden software for strain analysis.

Using gadolinium contrast material Dotarem (Gadoterate meglummine) 0.3 mmol per Kg.

Pediatric Use: a single dose of 0.1 mmol/kg (term neonates to 17 years).

Cardiac MR Examination:

Image analysis: The digital imaging and communications in medicine (DICOM) files were sent to a computer running specialized cardiac software:

Assessment of the ventricular volumes and function: Cine MRI was used in conjunction with commercially available software to extract global functional characteristics. Short-axis images were used to manually sketch the endocardial borders of both ventricles during systole and diastole. Heart end-diastolic and end-systolic volumes were calculated using Simpson's rule. Following this, measurements for EDV and ESV were used to determine

stroke volume (SV) and ejection fraction (EF). A normal ventricular ejection fraction is defined as 55-75%, whereas an intermediate range is 40-54% and a low range is 40%.

Evaluation of T1 mapping and myocardial ECV: Short-axis T1 mapping images were manually assessed**.** According to the 17 cardiac segments model, a ROI >12 pixels was drawn on the pre-contrast images in each segment of the basal, mid-ventricular and apical cuts, excluding the apex, giving a total of 16 segments in each patient.

On the after-contrast photos, a ROI was made over the same area. To get the signal reduction of the blood, a ROI was made in the blood pool in both the pre- and post-contrast pictures. The LGE pictures were ignored while those ROIs were drawn blindly.

Figure (1): Pre (A) and post (B) contrast T1 mapping images showing ROI drawn in the six basal segments; anterior, antero-septal (AS), infero-septal (IS), inferior, infero-lateral (IL) and antero-lateral (AL) segments as well as the blood pool.

Assessment of associated myocardial scarring: By the FWHM LGE quantification method on the segment workstation: a region of interest was drawn to encompass roughly the hyper-enhanced region, and then an arrangement of threshold (20–50%) values was tested to determine the optimal value.

Feature tracking myocardial strain analysis: Post-processing with the use of specialized commercially available software allowed for the derivation of circumferential,

longitudinal, and radial myocardial strain analyses of the various myocardial segments from the usual short axis cine pictures. It's a quantitative measure of the contractility of individual chambers in the heart.

Assessment of associated congenital anomalies: Using multi-planar and multi-sequence imaging to examine the heart's structure and function thoroughly.

Statistical analysis of the data: The data was fed to the computer and analyzed using IBM SPSS software package version 20.0. (Armonk, NY: IBM Corp.). Qualitative data were described using numbers and percentages. The Shapiro-Wilk test was used to verify the normality of the distribution. Quantitative data were described

using range (minimum and maximum), mean, standard deviation, median and interquartile range (IQR). The significance of the obtained results was judged at the 5% level.

One-way ANOVA test For normally distributed quantitative variables to compare between more than two groups, and a post hoc test (Tukey) for pairwise comparisons.

3. Results

T1 mapping

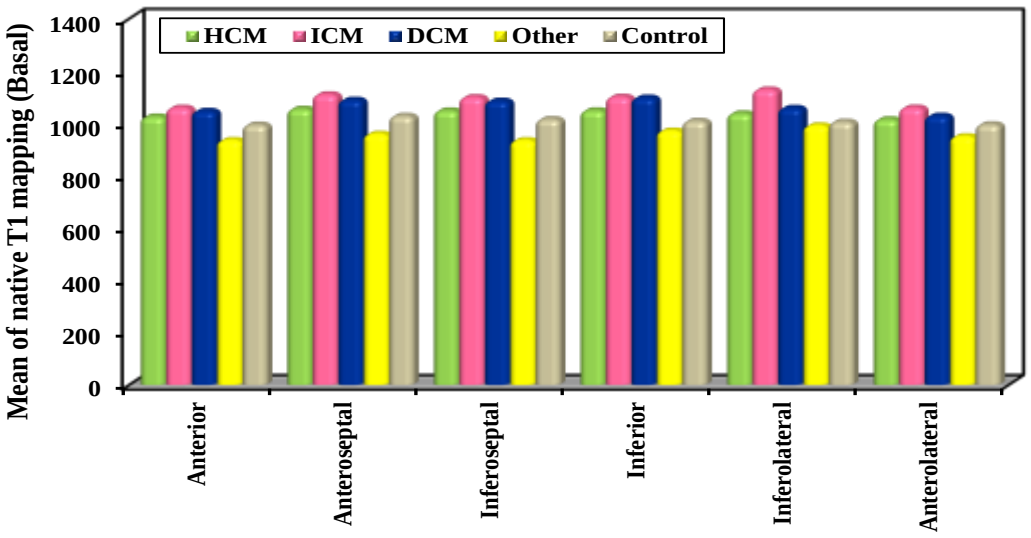

Figure (2): Comparison between the different studied groups according to Native T1 mapping (Basal)

-Significant T1 mapping values at basal inferior segments of the dilated cardiomyopathy group in comparison with controls (Min-Max 1043.0 – 1180.0, Mean ± SD 1098.3 ± 35.38, Median (IQR) 1096.5 (1067.0–1130.0)) and p-value 0.049 **(Statistically significant at p ≤ 0.05)**

-Significant T1 mapping values at basal inferior segments in the ischemic cardiomyopathy group in comparison with controls (Min-Max 864.0 – 1354.0, Mean ± SD 1101.2 ± 108.5, Median (IQR) 1071.0(1031.0–1150.5)) and p-value 0.047 **(Statistically significant at p ≤ 0.05)**

-Significant T1 mapping values at basal inferolateral segments in the ischemic cardiomyopathy group in comparison with controls (Min-Max 1011.0 – 1590.0, Mean ± SD 1129.2 ± 129.2, Median (IQR) 1098.0(1046.0–1135.0)) and p-value 0.005 **(Statistically significant at p ≤ 0.05)**

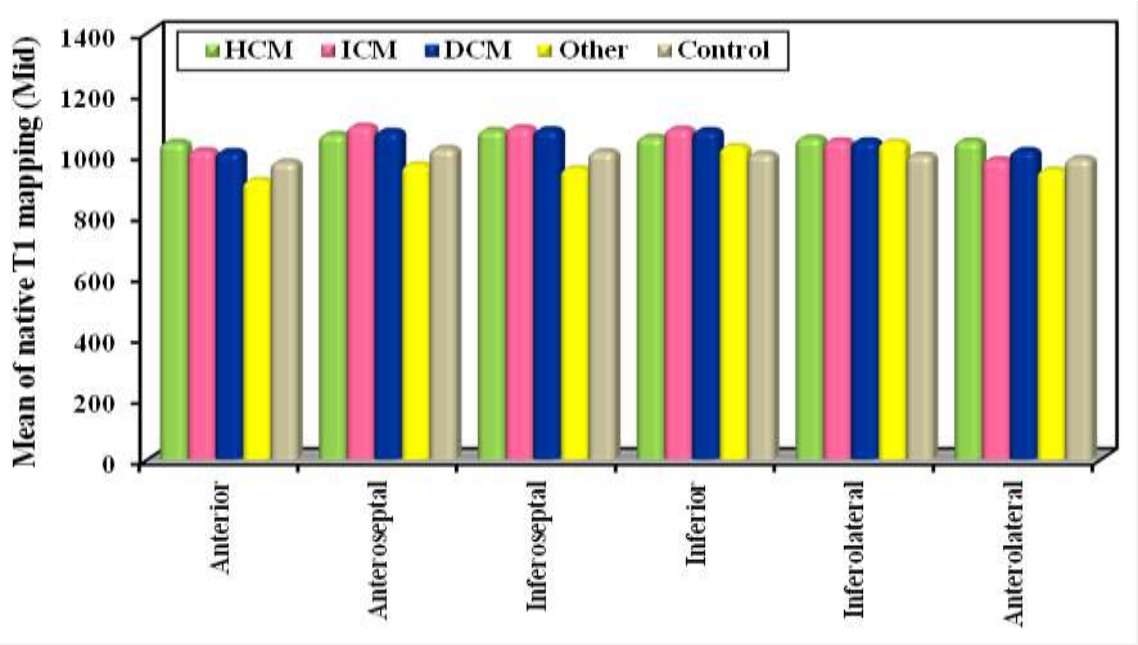

Figure 3: Comparison between the different studied groups according to Native T1 mapping (Mid)

-Significant T1 mapping values at mid-inferoseptal segments in the ischemic cardiomyopathy group in comparison with controls (Min-Max 996.0 – 1322.0, Mean ± SD 1088.3 ± 77.12, Median (IQR) 1082.0 (1027.5–1131.0)) and p-value 0.037 **(Statistically significant at p ≤ 0.05)**

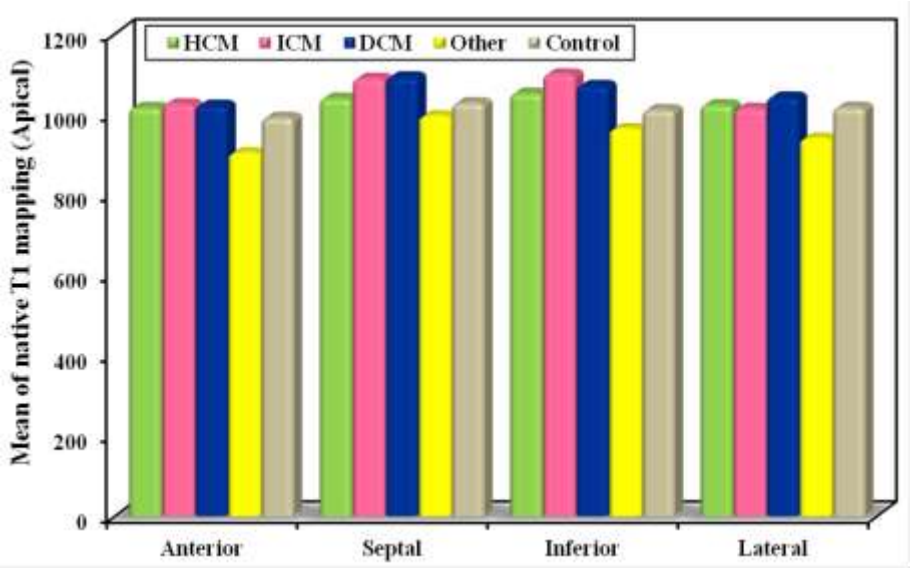

Figure (4): Comparison between the different studied groups according to Native T1 mapping (Apical)

There is no evidence of significant T1 mapping segmental values in any of the cardiomyopathy groups.

Strain analysis

Table (1): Comparison between the different studied groups according to Global circumferential strain:

Global Circumferential strain	**HCM (n = 31)**	**ICM (n = 27)**	**DCM (n = 30)**	**Others (n = 12)**	**Control (n = 30)**
Min. – Max.	-29.98 – -10.51	-14.47 – -5.26	-15.90 – -3.24	-23.17 – -8.15	-26.20 – -17.08
Mean ± SD.	-23.05 ± 5.39	-8.87 ± 2.62	-8.87 ± 3.53	-16.38 ± 4.75	-21.33 ± 2.44
Median (IQR)	-25.11 (-27.39– -19.99)	-8.16 (-10.86 – -7.05)	-8.01 (-10.25 – -5.95)	-17.84 (-19.20 – -13.74)	-20.98 (-23.35 – -19.72)
p	**0.406**	**<0.001***	**<0.001***	**0.002***	

-Significant global circumferential strain analysis values in the ischemic cardiomyopathy group in comparison with controls (Min-Max -14.47 – -5.26, Mean ± SD -8.87 ± 2.62, Median (IQR) -8.16 (-10.86 – -7.05)) and a p-value <0.001 (**Statistically significant at p ≤ 0.05)**

-Significant global circumferential strain analysis values in the dilated cardiomyopathy group in comparison with controls (Min-Max -15.90 – -3.24, Mean ± SD -8.87 ± 3.53, Median (IQR) -8.01 (-10.25 – -5.95)) and a p-value <0.001 (**Statistically significant at p ≤ 0.05)**

-Significant global circumferential strain analysis values in others cardiomyopathy group in comparison with controls (Min-Max -23.17 – -8.15, Mean ± SD -16.38 ± 4.75, Median (IQR) -17.84(-19.20 – -13.74)) and a p-value of 0.002 (**Statistically significant at p ≤ 0.05)**

Table (2): Comparison between the different studied groups according to Global radial strain:

Global Radial strain	**HCM (n = 31)**	**ICM (n = 27)**	**DCM (n = 30)**	**Other (n = 12)**	**Control (n = 30)**
Min. – Max.	13.03 – 75.81	7.61 – 27.20	6.27 – 41.80	-0.49 – 60.11	29.82 – 58.34
Mean ± SD.	38.05 ± 14.22	17.29 ± 4.95	16.79 ± 6.74	25.17 ± 17.19	42.63 ± 7.88
Median (IQR)	37.49 (27.65 – 46.59)	16.61 (14.0 – 19.86)	16.37 (13.21 – 19.66)	29.12 (12.49 – 34.34)	40.57 (36.86 – 46.34)
p	**0.408**	**<0.001***	**<0.001***	**<0.001***	

-Significant global radial strain analysis values in the ischemic cardiomyopathy group in comparison with controls (Min-Max 7.61 – 27.20, Mean ± SD 17.29 ± 4.95, Median (IQR) 16.61(14.0 – 19.86)) and p-value <0.001 (**Statistically significant at p ≤ 0.05)**

-Significant global radial strain analysis values in the dilated cardiomyopathy group in comparison with controls (Min-Max 6.27 – 41.80, Mean ± SD 16.79 ± 6.74, Median (IQR) 16.37(13.21 – 19.66)) and p-value <0.001 (**Statistically significant at p ≤ 0.05)**

-Significant global radial strain analysis values in others cardiomyopathy group in comparison with controls (Min-Max -0.49 – 60.11, Mean ± SD 25.17 ± 17.19, Median (IQR) 29.12(12.49 – 34.34)) and p-value <0.001 (**Statistically significant at p ≤ 0.05)**

Table 3: Comparison between the different studied groups according to Global longitudinal strain:

Global Longitudinal strain	**HCM (n = 31)**	**ICM (n = 27)**	**DCM (n = 30)**	**Other (n = 12)**	**Control (n = 30)**
Min. – Max.	-22.04 – -4.53	-12.66 – -3.06	-16.43 – -3.50	-16.64 – -7.35	-22.77 – -14.93
Mean ± SD.	-13.37 ± 3.99	-7.72 ± 3.07	-9.41 ± 3.26	-12.74 ± 3.40	-19.22 ± 1.85
Median (IQR)	-13.25 (-15.62 – -10.70)	-7.31 (-10.23 – -5.49)	-8.69 (-10.69 – -7.45)	-13.82 (-15.32 – -9.01)	-19.01 (-20.56 – -17.88)
p	**<0.001***	**<0.001***	**<0.001***	**<0.001***	

-Significant global longitudinal strain analysis values in the hypertrophic cardiomyopathy group in comparison with controls (Min-Max -22.04 – -4.53, Mean ± SD -13.37 ± 3.99, Median (IQR) -13.25(-15.62 – -10.70)) and p-value <0.001 (**Statistically significant at p ≤ 0.05)**

-Significant global longitudinal strain analysis values in the ischemic cardiomyopathy group in comparison with controls (Min-Max -12.66 – -3.06, Mean ± SD -7.72 ± 3.07, Median (IQR) -7.31(-10.23 – -5.49)) and p-value <0.001 (**Statistically significant at p ≤ 0.05)**

-Significant global longitudinal strain analysis values in the dilated cardiomyopathy group in comparison with controls (Min-Max -16.43 – -3.50, Mean ± SD -9.41 ± 3.26, Median (IQR) -8.69(-10.69 – -7.45)) and p-value <0.001 (**Statistically significant at p ≤ 0.05)**

-Significant global longitudinal strain analysis values in others cardiomyopathy group in comparison with controls (Min-Max -16.64 – -7.35, Mean ± SD -12.74 ± 3.40, Median (IQR) -13.82(-15.32 – -9.01)) and p-value <0.001 (**Statistically significant at p ≤ 0.05)**

Case 1

History: 43-year-old male known to have dilated CM. He complains of SOB, and TTE showed a dilated LV with impaired systolic function (LVEF= 30%).

CMR findings:

A case of non-ischemic dilated cardiomyopathy (DCM) showing a dilated LV with severely impaired systolic function. EF = 30 %, no intra-cardiac thrombi or MVO are noted, no detected myocardial fibrosis, average-sized RV with preserved systolic function, EF = 67%

Detection of EDV, ESV and EF:

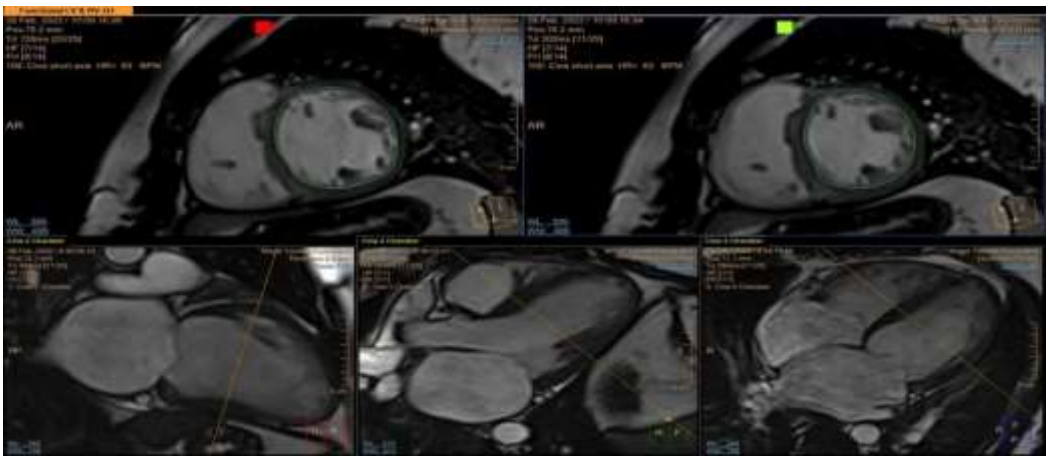

Figure (5): Post-processing by Philips workstation of LV for detection of EDV, ESV and EF (Drawing endo contour of the left ventricle short-axis images at end diastole and end systole, then repeating this step for each slice in the ED window (left-hand side) and each slice in the ES window (right-hand side))

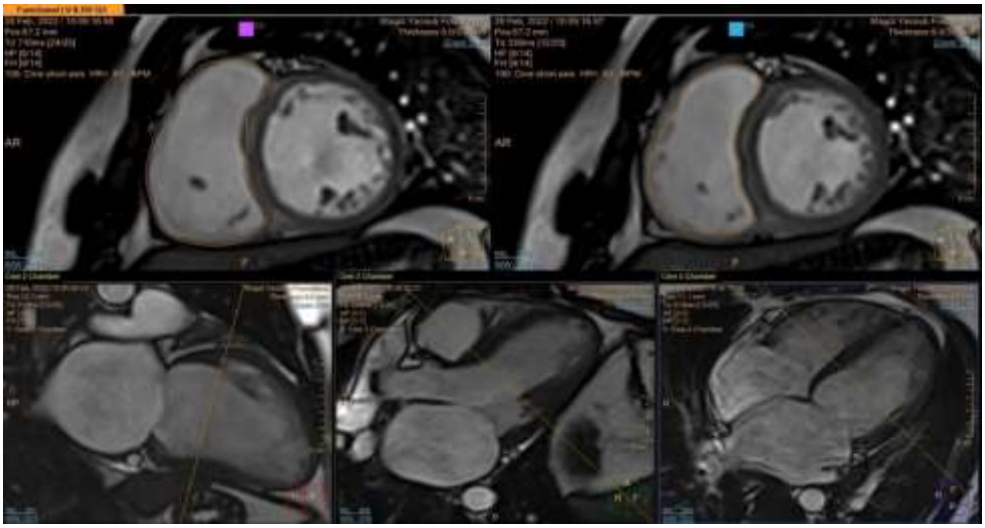

Figure (6): Post-processing by using Philips workstations for RV for detection of EDV, ESV and EF (Drawing the endo contour of the right ventricle short-axis images at end diastole and end systole, then repeating this step for each slice in the ED window (left-hand side) and each slice in the ES window (right-hand side))

The results were:

Table (4): Cardiac function, EDV, ESV& EF values

Ventricle/ volume	EF (%)	EDV (ml)	ESV (ml)	SV (ml)	EDVI (ml/m2)	ESVI (ml/m2)	SVI (ml/m2)
RV	67	127	42	85	65	21	43
LV	**30**	**286**	**201**	85	**145**	**102**	43
CO = 5.7 L/min			HR = 67 b/min				

Detection of native T1 mapping and ECV:

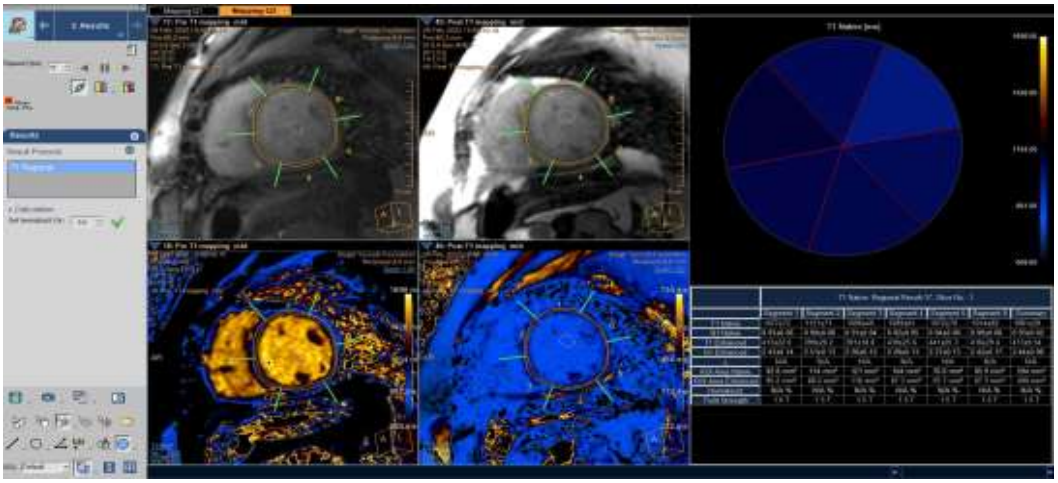

Figure (7): Post-processing by using Philips workstation for detection of T1 mapping and ECV at basal level (Drawing myocardial borders at basal level, endo contour, epi contour and blood contour, then creating spoke wheels of 6 segments and entering the HCT value)

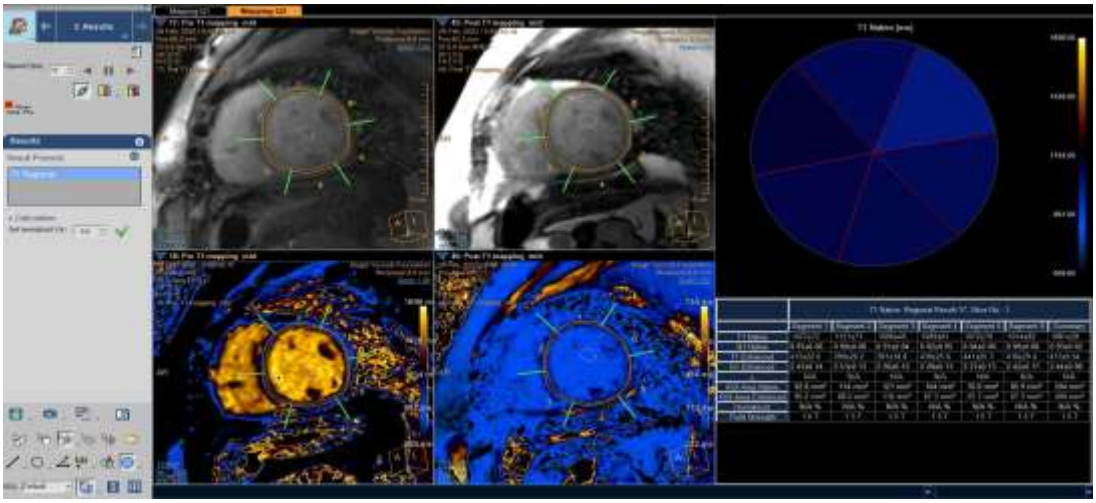

Figure (8): Post-processing by using Philips workstation for detection of T1 mapping and ECV at mid-level (Drawing myocardial borders at mid-level endo contour, epi contour and blood contour, then creating spoke wheels of 6 segments and entering HCT value)

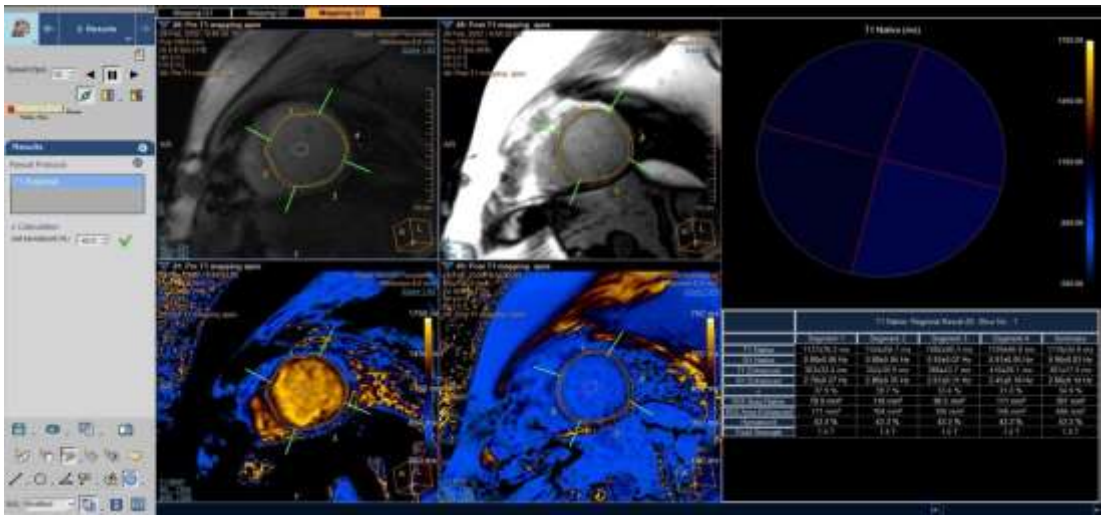

Figure (9): Post-processing by using Philips workstation for detection of T1 mapping and ECV at the apical level (Drawing myocardial borders at the apical level, endo contour, epi contour and blood contour, then creating spoke wheels of 4 segments and entering the HCT value)

The results were:

Table (5): Native T1 mapping and ECV segmental values

Hematocrit value=40.1		**Anterior (msec)**	**Antroseptal (msec)**	**Infroseptal (msec)**	**Inferior (msec)**	**Anterolateral (msec)**	**Anterolateral (msec)**
Basal	**Native T1**	1073±68.2	1115±42.7	1137±50.1	1115±84.	1038±65.2	1033±73.5 ms
	ECV	29.4 %	29.7 %	31.6 %	31.3 %	25.5 %	27.3 %
Mid	**Native T1**	1076±54.0 ms	1130±40.5 ms	1131±48.4 ms	1105±63. 2 ms	1059±44.8 ms	1006±56.8 ms
	ECV	30.9 %	32.0 %	33.1 %	31.4 %	26.0 %	26.5 %
Apical	**Native T1**	1067±64.3	1131±33.0 ms		1098±55.	1050±65.4 ms	
	ECV	29.5 %	30.5 %		29.3 %	28.8 %	

Detection of Strain Analysis

First, set the end-systolic phase to select the slices we are going to work on

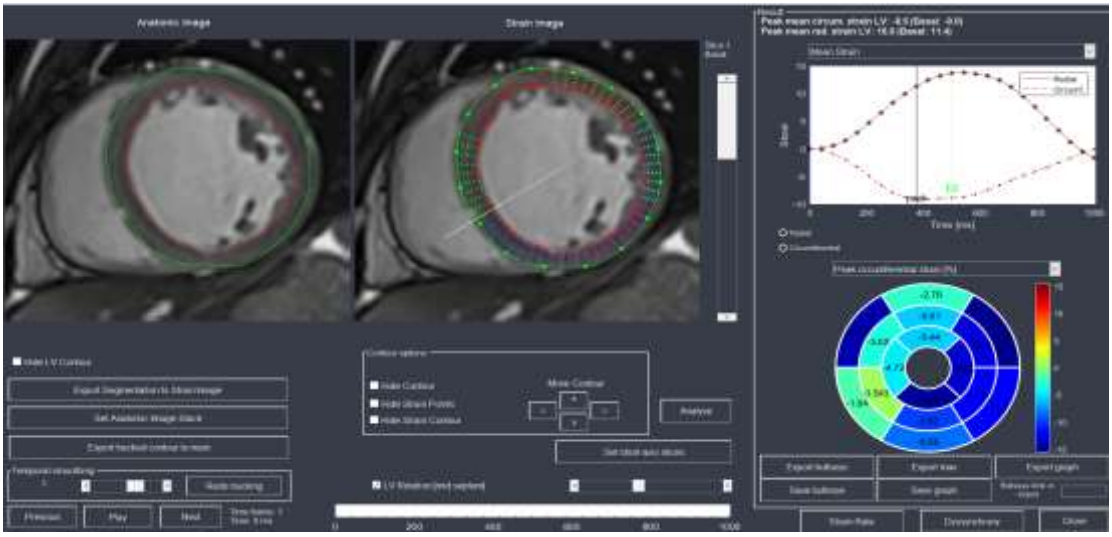

Figure (10): Post-processing using Segment software for detection of circumferential and radial strain analysis at basal level. Results of circumferential and radial strain after drawing endo contours in red and epi contours in green at the LV basal level

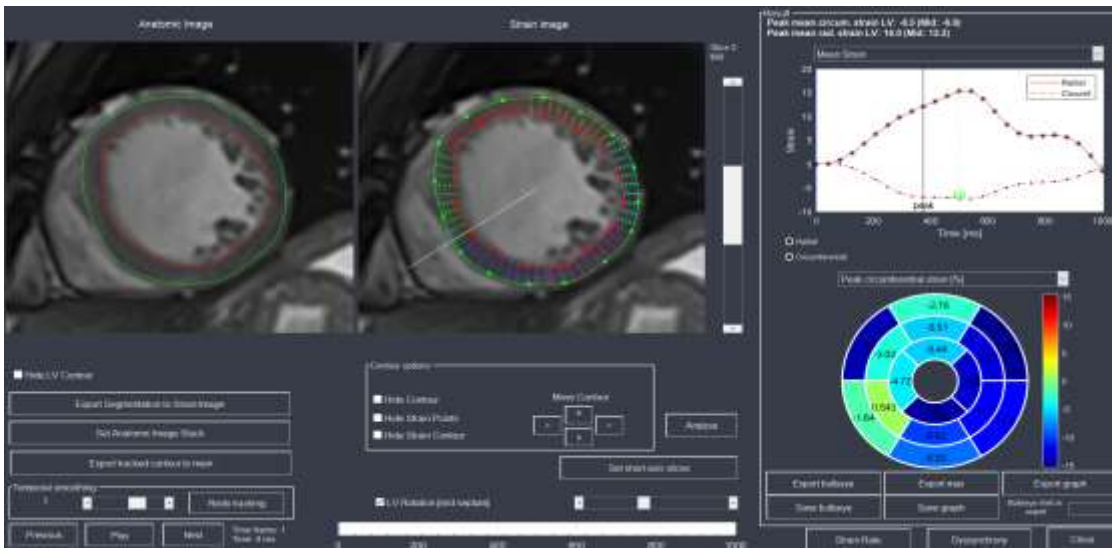

Figure (11): Post-processing using Segment Workstation for detection of circumferential and radial strain analysis at mid-level. Results of circumferential and radial strain after drawing endo contours in red and epi contours in green at LV mid-level

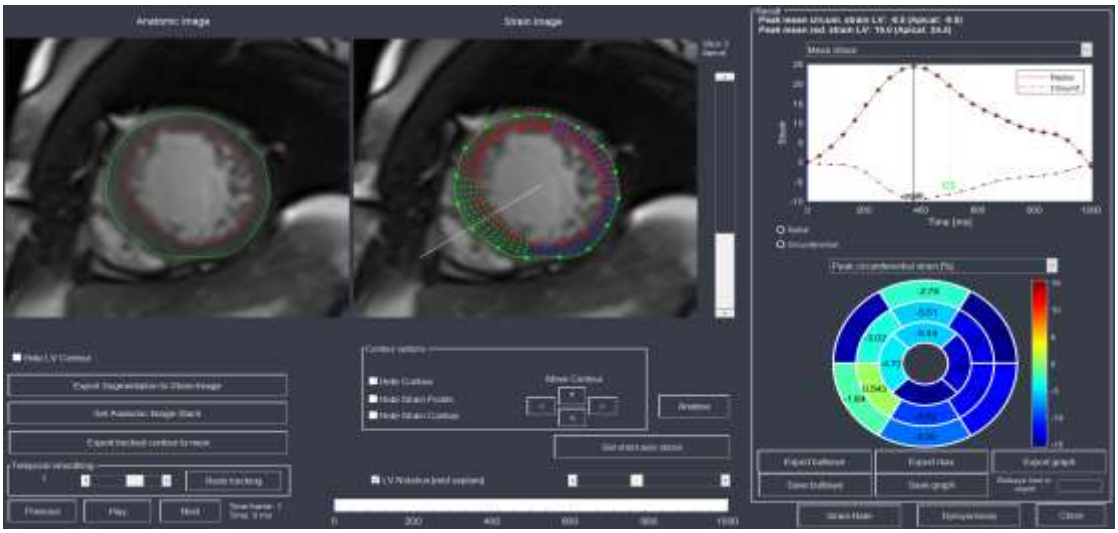

Figure (12): Post-processing using Segment workstation for detection of circumferential and radial strain analysis at the apical level. Results of circumferential and radial strain after drawing endo contours in red and epi contours in green at the LV apical level

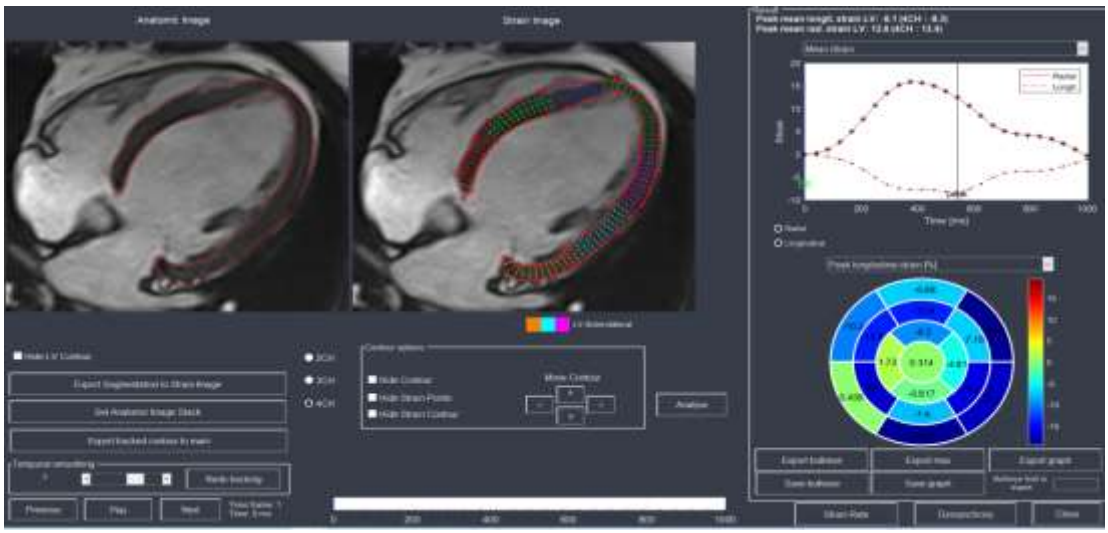

Figure (13): Post-processing using Segment workstation for detection of longitudinal strain analysis at 4ch. Results of longitudinal strain after drawing endo and epi contours with only the red color of the LV at 4 ch

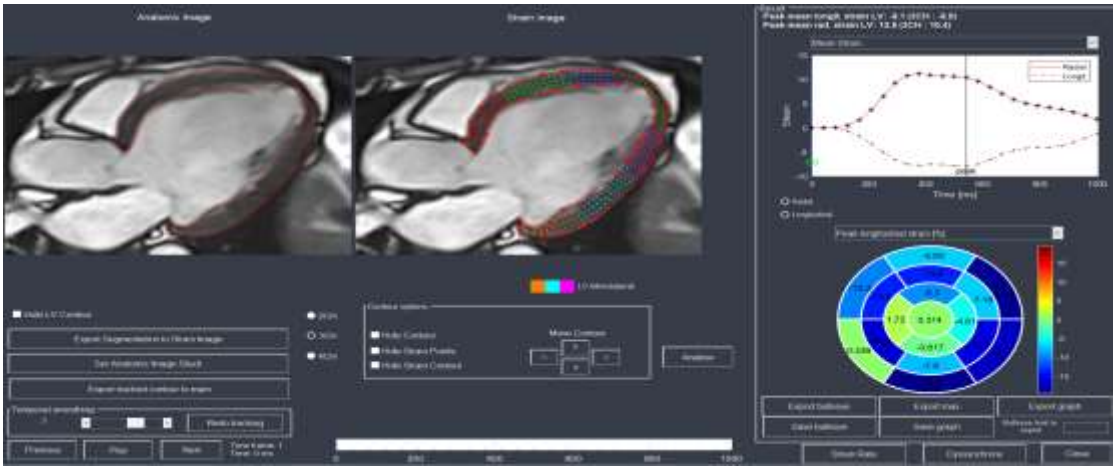

Figure (14): Post-processing using Segment Workstation for detection of longitudinal strain analysis at 3 ch. (Results of longitudinal strain after drawing endo and epi contours with the red color only of the LV at 3 ch)

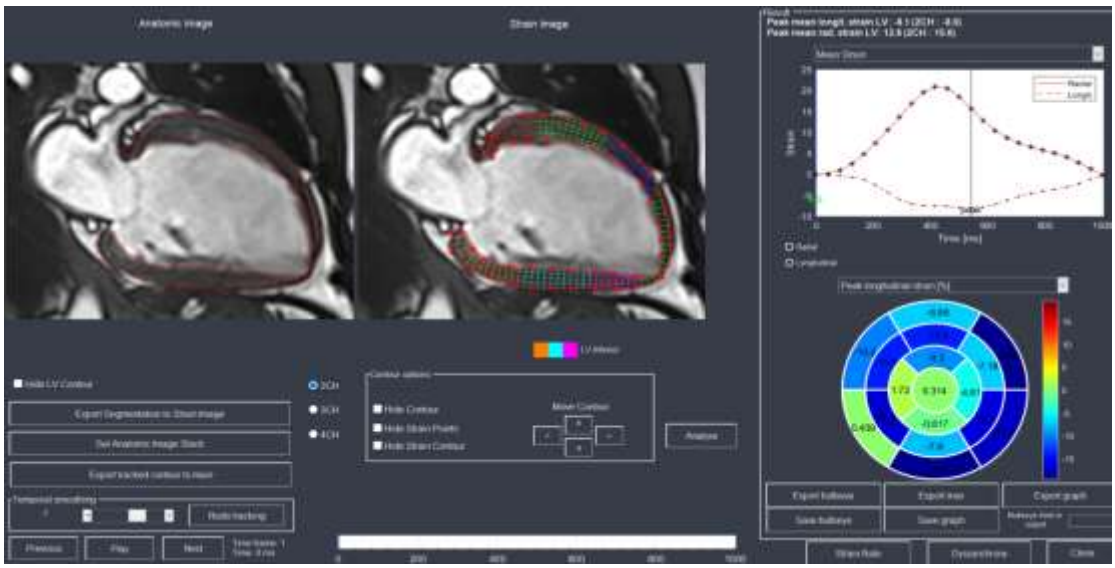

Figure (15): Post-processing using Segment Workstation for detection of longitudinal strain analysis at 2 ch. (Results of longitudinal strain after drawing endo and epi contours with only the red color of the LV at 2 ch)

The results were:

Table (6): Global Strain Analysis Values:

Global Circumferential Strain	**-8.5**
Global Radial Strain	**16**
Global Longitudinal Strain	**-8.1**

Clinical use of T1 mapping and ECV

Hypertrophic cardiomyopathy

Native T1 values are prolonged in HCM and correlate with wall thickness, suggesting that it is a marker of disease severity. **(4,5)** Patients with HCM have reduced post-contrast myocardial T1 consistent with diffuse interstitial fibrosis outside areas of LGE. ECV in HCM (29.1 ± 0.5% [1.5T]) **(6)** in segments without LGE has been shown to be in the upper normal range of normal patients'. Fig. 16.a **(7)** ECV can be used in the differential diagnosis of HCM vs. athletic remodeling in the athlete's heart, particularly in those subjects in the grey zone of LV wall thickness (12–15 mm). Whereas ECV increases with increasing LV hypertrophy in HCM (due to extracellular matrix expansion and myocardial disarray), ECV reduces in athletes with increasing wall thickness (due to an increase in healthy myocardium by cellular hypertrophy). **(7)** The impact of myocardial disarray on T1 mapping in HCM remains controversial and may result in an overestimation of ECV. **(8)**

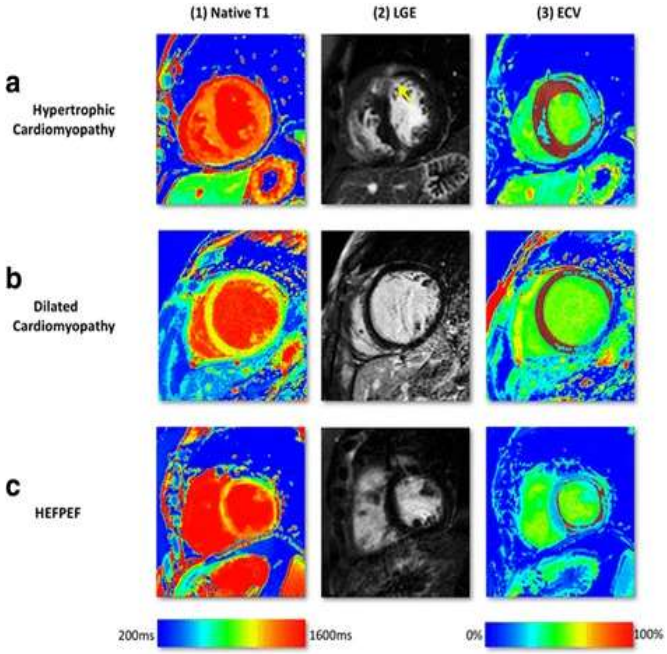

Fig. 16. Multi-parametric tissue characterization at mid-slice in cardiomyopathies. On ECV-maps, *red areas* represent ECV greater than 30%. T1-mapping was done using a modified Look-Locker Inversion Recovery (MOLLI) pulse sequence on a 1.5 Tesla Ingenia, Philips, Best, The Netherlands. **a** HCM showing diffuse and heterogeneous LGE in the anterior wall (*yellow arrow*, a2). Native T1 was diffusely raised, exceeding the hypertrophied segments (a1). ECV-maps demonstrate higher ECV in and around the diffuse LGE (a3). **b** DCM with no LGE enhancement (b2) but raised native T1 values in the septum (1000–1200 ms) (b1) and raised ECV (b3). **c** HFpEF Native-T1 values were significantly raised through-out (>1000 ms) with no presence of scar on LGE-imaging (c2). ECV maps demonstrated a patchy rise in extracellular space (c3). Abbreviations: DCM, dilated cardiomyopathy; ECV, extracellular volume; HFpEF, heart failure with preserved ejection fraction; HCM, hypertrophic cardiomyopathy; LGE, Late Gadolinium Enhancement

Dilated cardiomyopathy

Native T1 values are prolonged in DCM and correlate with reduced wall thickness **(4,5)**. ECV measurement reflects myocardial collagen content in DCM and might serve as a non-invasive imaging biomarker to monitor therapy response and aid risk stratification in different stages of DCM **(9).** ECV in DCM is in a similar range to HCM ($28 \pm 0.4\%$[1.5T]). Fig.16.b **(6)** The pathophysiologies that correlate and are responsible for the similar ECV values in DCM and HCM are not fully understood, but since DCM and HCM can usually be distinguished by their distinct ventricular geometry, the overlap in ECV is clinically irrelevant. Furthermore, ECV elevation is typically pronounced in the mid-wall sections in DCM compared with RV hinge points and hypertrophied segments in HCM

Clinical use of myocardial strain analysis

The clinical application of myocardial strain imaging has been increasingly assessed over the past few years.

The study of myocardial strain reveals fresh information about the disease's mechanisms:

Intramural functional abnormalities in patients with hypertrophic cardiomyopathy have been shown to extend beyond the presence of LGE, as intramural systolic strain is abnormal in hypertrophied segments compared to segments without hypertrophy, regardless of the presence of LGE. However, multiple investigations have found a linear relationship between myocardial strain and the amount of LGE, both at the global and segmental levels leading to the conclusion that strain analysis could be used in the future to indirectly detect the presence of scar without the requirement of a contrast agent. **(10)**

In patients with hypertrophic cardiomyopathy, both fibrosis and hypertrophy contribute to aberrant cardiac mechanics (HCM). Endocardial dysfunction is caused by increased wall stress and relative endocardial ischemia, as well as fibrotic alterations, resulting in a significant drop in GLS. **(11)**

As a result, GLS (Global Longitudinal Strain) can be utilized to distinguish pathological hypertrophy from physiological hypertrophy in trained athletes' conditioned hearts, which have normal GLS values. Longitudinal septal strain, in particular, was found to be negatively associated with histopathological fibrotic alterations and a more powerful indicator of arrhythmia than late gadolinium enhancement. In adults with HCM, GLS has also been proven to predict adverse outcomes. Endocardial dysfunction causes GRS (Global Radial Strain) to be depressed in HCM patients; yet, due to epicardial layer thickening, these patients frequently have elevated LVT and delayed LV untwist. **(11)**

Patients with HCM have lower longitudinal, radial, and circumferential strain than control participants, according to FT-CMR findings, with radial and longitudinal strain being able to predict clinical prognosis. **(11)**

Regardless of RV size and function, global and regional right ventricular (RV) strain metrics have been reported to be compromised in individuals with arrhythmogenic right ventricular cardiomyopathy (ARVC). **(11)**

Similarly, strain parameters have been demonstrated to be affected in patients with acute or prior myocarditis and retained LVEF independent of LGE, validating CMRFT's better sensitivity in detecting contractile damage at a preclinical stage. **(11)**

We discovered that in patients with LV noncompaction, subclinical myocardial deformation begins early in the disease's natural history, manifesting as a reduction in all global strain indices as early as childhood. In contrast LVEF decline tends to emerge later in adulthood. **(11)**

4. Discussion:

Our study was conducted on 130 cases, 100 of them were diagnosed to have cardiomyopathy by echocardiography, and 30 as a control.

We grouped them as 30 patients in the DCM group, 27 patients in the ICM group, 31 patients in the HCM group, and 12 patients from other types (RCM, ARVD, and LVNC) in others group.

After Image and statistical analysis, our results revealed a description of the relation between the segmental myocardial T1 mapping and ECV as well as strain analysis in the three different directions (global peak mean circumferential strain analysis, global peak mean radial strain analysis, and global peak mean longitudinal strain analysis) in different types of cardiomyopathies versus control subjects, except for ECV (no control subjects- see study limitations).

T1 quantification was performed with a modified Look-Locker Inversion Recovery (MOLLI) sequence acquired pre- and 15 minutes following bolus contrast administration in short-axis images with variable inversion preparation time. All images were acquired during the same cardiac phase at late diastole using the same imaging parameters.

Image analysis:

Images (DICOM) were transferred to a workstation with a dedicated cardiac software package for further analysis.

After Statistical analysis, we found that Statistically significant T1 mapping values at basal inferior, basal inferolateral and mid inferoseptal segments in the ICM group and basal inferior segments in the DCM group.

This means that myocardial T1 native provides the greatest distinction between healthy myocardium and diseased tissue. As such, it bears the potential for the development of an easy-to-implement test in patients with suspected diffuse fibrosis, which may be missed by classic LGE imaging. Furthermore, in subjects with low pre-test likelihood for cardiomyopathy or those in whom contrast administration is contraindicated, it may serve as a practical screening test. Future advances in sequence development that would provide whole-heart coverage might derive a useful approach to characterizing regional differences and potentially obviate the need for contrast administration. The observed findings in myocardial T1 native emphasize several important aspects of post-contrast T1 mapping. Because gadolinium administration greatly shortens T1 values, the overall T1 tissue relaxation will depend on the dose and relaxivity of the gadolinium contrast agent, the intrinsic T1 values of the tissue, and the timing of the acquisition and bioavailability after gadolinium administration. Post-contrast T1

sampling can thus be affected by various independent variables, including renal function, contrast type and dose of administration, variation in sampling time points, and individual pharmacokinetics. Post-contrast T1 imaging at the rigid time points can prove cumbersome in clinical routine; we improved the inter-study comparability of the post-contrast T1 sampling by using consistent time points in our routine cardiomyopathy imaging protocol. Yet, the influences above might explain the lower performance of post-contrast T1 values and ECV.

This was in agreement with previous studies, as T1 mapping techniques provide quantifiable information on longitudinal relaxation by acquiring images with different inversion times and multiparametric curve-fitting analysis. T1 maps are derived as parametric reconstructed images, in which the signal intensity of a pixel depends on the absolute longitudinal relaxation properties of this voxel **(12).** Several methodologies were tested to acquire the myocardial T1 relaxation values, including sets of saturation or inversion recovery images with varying inversion times and, lately, the classical and modified Look-Locker sequences **(13).** The variant of the latter sequence, also applied in the present study, leads to a series of multiple images acquired within the same phase of the cardiac cycle through a selective fixed delay over successive heartbeats. Some studies using this or related methodologies suggested that myocardial T1 native values could be used to discern post-infarct scar from healthy myocardium. Most of these studies, however, focused on the post-contrast T1 values and reported significantly shorter T1 times compared with controls **(13).** In a population of patients with mixed causes of heart failure, Iles et al. reported shorter post-contrast T1 compared with controls, even when excluding areas of regional fibrosis **(14).** These investigators also observed an inverse relationship between post-contrast T1 values and the amount of fibrosis on histology. The ability of T1 imaging to quantify the amount of diffuse fibrosis was also confirmed using a novel technique of ECV imaging derived from continuous infusion **(15).** Diastolic myocardial impairment, an indirect marker of diffuse myocardial fibrosis, was shown to correlate with abnormal post-contrast T1 values in patients with heart failure, diabetic cardiomyopathy, and amyloidosis **(16).** The observed changes in post-contrast T1 values have been previously related to an increase in extracellular space and well described in models of acute and chronic ischemic or inflammatory myocardial injury. The physiological correlation between diffuse myocardial pathology and observed increases in native T1 is less well understood. Extracellular matrix remodeling is orchestrated by fibroblasts within the heart, but changes in

extracellular matrix composition affect cardiomyocyte survival **(17).** Image analysis for feature tracking myocardial strain analysis: Circumferential, longitudinal and radial myocardial strain analysis of the different myocardial segments were derived from the routine short-axis cine images by post-processing with the aid of special commercially available software. It acts as a quantitative assessment of segmental myocardial contractility.

And after Statistical analysis, we found statistically significant global Peak mean Circumferential, Radial and Longitudinal strain analysis in the ICM, DCM and Others) groups and only global peak mean longitudinal strain analysis in the HCM group.

Our findings provide a novel and easy-to-use method for the detection of diffusely diseased myocardial tissue by CMR with an immediate potential for clinical translation. The authors examined myocardial deformation indices using feature-tracking cardiac magnetic resonance (FT-CMR) in patients with different types of cardiomyopathies suffering from variable degrees of myocardial affection in terms of contractility disorders and scarring. The feasibility of using strain analysis by CMR for quantitative detection of regional myocardial motion abnormalities, contractility disorders and scarring.

Segmental strain analysis by feature-tracking cardiac magnetic resonance (FT-CMR) showed good capability in the assessment of myocardial scarring and contractility disorders in different cases of cardiomyopathy and enabled myocardial deformation analysis without lengthening the imaging protocol or the timing of the CMR examination.

This was in agreement with previous studies, as during cardiac contraction, vectors in the radial, circumferential, and longitudinal directions may be used to describe myocardial deformation. Positive strain values are recorded in the radial direction owing to thickening in the radial direction during ventricular contraction, while negative strain values are found in the circumferential and longitudinal directions during systole **(18)**. Following the various directions in which the myocardium deforms may be used to determine the longitudinal, circumferential, and radial strain. The longitudinal shortening from the base to the apex is measured by longitudinal strain, which is a negative metric. Radial strain is the radially directed myocardial deformation towards the LV cavity's center, which represents LV thickening and thinning motion throughout the cardiac cycle; positive values indicate thickening and thinning motion. Circumferential strain is the shortening of LV myocardial fibers around the circular perimeter as viewed from a short-axis perspective, and it is denoted by a negative sign **(19)**. In the last two decades, various

techniques for assessing global and local myocardial deformation, such as myocardial tagging, tissue displacement encoding with stimulated echoes, and strain-encoded imaging, have evolved **(18)**. All of these approaches, with myocardial tagging as the gold standard for assessing myocardial strain, have one thing in common: sequences must be obtained in addition to an already lengthy clinical protocol. Using routinely obtained steady-state free precession (SSFP) cine sequences as input, myocardial feature tracking (FT) was introduced for myocardial strain assessment. Myocardial boundaries can be recognized and the movement of myocardial segments tracked during the cardiac cycle using optical flow methods or non-rigid image registration and segmentation algorithms **(18).**

5. Limitations:

There are many study limitations that must be acknowledged, some of which are that it is a relatively new technique with few similar studies to compare it with and an unequal gender distribution with more males included in the study.

ECV control results cannot be obtained as health volunteers aren't obligated to undergo contrast injection according to the health volunteer protocol in AHC.

Also, ECV for some patient cases cannot be obtained due to the time factor in the determination of the HCT value and the cases obtained in a period lasting up to one and a half years.

More studies with a larger number of patients may be needed for confirmation of our results. Also being a retrospective study.

6. Conclusion:

T1 mapping and feature-tracking cardiac magnetic resonance are good at assessing myocardial scarring and contractility disorders in different types of cardiomyopathy. They also make it possible to do quantitative analysis of myocardial deformation without making the imaging protocol or CMR exam longer. Previous studies have shown that this is an important sign of a myocardial disorder.

7. Abbreviations:

AHA/The American Heart Association

ARVC/Arrhythmogenic Right Ventricular Cardiomyopathy

CMP /Cardiomyopathy

CMR/Cardiovascular Magnetic Resonance

DCM/ Dilated Cardiomyopathy

ECG /Electrocardiography

ECV /Extra-cellular volume

EDV/End Diastolic Volume

EF/Ejection Fraction

ESV/End Systolic Volume

FT-CMR/Feature Tracking Cardiac MRI

GCS /Global Circumferential Strain

GLS/Global Longitudinal Strain

GRS /Global Radial Strain

HCM/Hypertrophic Cardiomyopathy

ICM/Ischemic Cardiomyopathy

IQR /interquartile range

IR/Inversion-Recovery

LGE/Late Gadolinium Enhancement

LV/Left Ventricle

LVH/Left Ventricular Hypertrophy

LVEDVI/Indexed Left Ventricle End Diastolic Volume

LVESVI/Indexed Left Ventricle End Systolic Volume

LVNC/Left Ventricular Non-Compaction

LVSVI/ Indexed Left Ventricle Stroke Volume

MOLLI/ Modified Look-Locker Inversion Recovery

MRI/ Magnetic Resonance Imaging

RCM / Restrictive Cardiomyopathy

ROI/ Region Of Interest

RV/ Right Ventricle

RVEF/ Right Ventricular Ejection Fraction

SCD/Sudden Cardiac Death

SD/Standard Deviation

ShMOLLI/Shortened Modified Look-Locker Inversion Recovery

SI/Signal Intensity

SOB/shortness of breath

S/P/status post

SSFP/Steady-State Free Precession

SV/Stroke Volume

SVI /Stroke Volume Indexed

T1 /Longitudinal Relaxation Time

TEE /Trans Esophageal Echo

TI/ Inversion Time

VENC/Velocity Encoding

WMT/Wall Motion Tracking

WHO/The World Health Organization

8. References:

1. **Kramer M, Jörg B, Scott D, Raymond J, Eike N, Society for Cardiovascular Magnetic Resonance Board of Trustees Task Force on Standardized Protocols.** Standardized cardiovascular magnetic resonance (CMR) protocols 2013 update. Journal of Cardiovascular Magnetic Resonance. 2013; 15(1): 91.
2. **O'Donnell H, Suhny A, Vithaya C, Kibar Y, Ronan P, Ramon M, et al.** Cardiac MR imaging of nonischemic cardiomyopathies: imaging protocols and spectra of appearances. Radiology. 2012; 262(2): 403-422.
3. **Jan B, Steven D, Andrew M.** Clinical Cardiac MRI. Springer Science and Business Media. 2012.
4. **Puntmann VO, Voigt T, Chen Z, Mayr M, Karim R, Rhode K, Pastor A, Carr-White G, Razavi R, Schaeffter T, Nagel E.** Native T1 Mapping in Differentiation of Normal Myocardium From Diffuse Disease in Hypertrophic and Dilated Cardiomyopathy. JACC Cardiovasc Imaging. 2013;6:475–84.
5. **Dass S, Suttie JJ, Piechnik SK, Ferreira VM, Holloway CJ, Banerjee R, Mahmod M, Cochlin L, Karamitsos TD, Robson MD, Watkins H, Neubauer S**. Myocardial tissue characterization using

magnetic resonance non-contrast t1 mapping in hypertrophic and dilated cardiomyopathy. Circ Cardiovasc Imaging. 2012;5:726–33.

6. **Sado DM, Flett AS, Banypersad SM, White SK, Maestrini V, Quarta G, Lachmann RH, Murphy E, Mehta A, Hughes DA, McKenna WJ, Taylor AM, Hausenloy DJ, Hawkins PN, Elliott PM, Moon JC**. Cardiovascular magnetic resonance measurement of myocardial extracellular volume in health and disease. Heart. 2012;98:1436–41.
7. **Swoboda PP, McDiarmid AK, Erhayiem B, Broadbent DA, Dobson LE, Garg P, Ferguson C, Page SP, Greenwood JP, Plein S.** Assessing Myocardial Extracellular Volume by T1 Mapping to Distinguish Hypertrophic Cardiomyopathy From Athlete's Heart. J Am Coll Cardiol. 2016;67:2189–90.
8. **Todiere G, Aquaro GD, Piaggi P, Formisano F, Barison A, Masci PG, Strata E, Bacigalupo L, Marzilli M, Pingitore A, Lombardi M.** Progression of myocardial fibrosis assessed with cardiac magnetic resonance in hypertrophic cardiomyopathy. J Am Coll Cardiol. 2012;60:922–9.
9. **aus dem Siepen F, Buss SJ, Messroghli D, Andre F, Lossnitzer D, Seitz S, Keller M, Schnabel PA, Giannitsis E, Korosoglou G, Katus HA, Steen H.** T1 mapping in dilated cardiomyopathy with cardiac magnetic resonance: quantification of diffuse myocardial fibrosis and comparison with endomyocardial biopsy. Eur Heart J Cardiovasc Imaging. 2015;16:210–6.
10. **Scatteia, A, Baritussio, A, & Bucciarelli-Ducci, C.** Strain imaging using cardiac magnetic resonance. Heart Failure Reviews. 2017; 22(4): 465–476.
11. **Muser, D, Castro, S. A, Santangeli, P, & Nucifora G.** Clinical applications of feature-tracking cardiac magnetic resonance imaging. World Journal of Cardiology. 2018; 10(11): 210–221.
12. **Ulrike B, Timothy L, Christian S, Stephen S, Sergio U, Reza R, et al.** Interleaved T1 and T2 Relaxation Time Mapping for Cardiac Applications. Journal of Magnetic Resonance Imaging. 2009; 29:480 –487.
13. **Stefan K, Vanessa M, Erica D, Lowri E, Andreas G, Stefan N, et al.** Shortened Modified Look-Locker Inversion recovery (ShMOLLI) for clinical myocardial T1-mapping at 1.5 and 3 T within a 9-heartbeat breath hold. Journal of Cardiovascular Magnetic Resonance. 2010; 12(1): 69.
14. **Leah I, Heinz P, Arintaya P, Joshi C, Pelin A, Sandeep N, et al.** Evaluation of diffuse myocardial fibrosis in heart failure

with cardiac magnetic resonance contrast-enhanced T1 mapping. Journal of the American College of Cardiology. 2008; 52(19): 1574-80.

15. **Martin U, Abiola J, Li-Yueh H, Peter K, Andreas G, Anthony H, et al.** Extracellular volume imaging by magnetic resonance imaging provides insights into overt and sub-clinical myocardial pathology. European Heart Journal. 2012; 33(10): 1268-1278.
16. **Nathan M, Chia Y, Pierre C, David B, João A C.** Assessment of myocardial fibrosis with cardiovascular magnetic resonance. Journal of the American College of Cardiology. 2011; 57(8): 891-903.
17. **Barallobre-Barreiro J., Didangelos A., Schoendube F.A.**, **Drozdoy I., Yin X**. Proteomics Analysis of Cardiac Extracellular Matrix Remodeling in a Porcine Model of Ischemia-Reperfusion Injury. Circulation. 2012; 125(6): 789-802
18. **Polacin M, Karolyi M, Eberhard M, Gotschy A, Baessler B, Alkadhi H.** Segmental strain analysis for the detection of chronic ischemic scars in non - contrast cardiac MRI cine images. Scientific Reports. 2021; 1–11.
19. **Scatteia, A., Baritussio, A., & Bucciarelli-Ducci, C.** Strain imaging using cardiac magnetic resonance. Heart Failure Reviews. 2017; 22(4): 465–476.